Astron. Astrophys. 343, 883–893 (1999)

ASTRONOMY AND ASTROPHYSICS

Search for X-ray emission from bona-fide and candidate brown dwarfs

R. Neuhäuser[1], C. Briceño[2], F. Comerón[3], T. Hearty[1], E.L. Martín[4], J.H.M.M. Schmitt[5], B. Stelzer[1], R. Supper[1], W. Voges[1], and H. Zinnecker[6]

[1] MPI für Extraterrestrische Physik, Giessenbachstrasse 1, D-85740 Garching, Germany
[2] Yale University, Department of Physics, New Haven, CT 06520-8121, USA
[3] European Southern Observatory, Karl-Schwarzschild-Strasse 2, D-85748 Garching, Germany
[4] Astronomy Department, University of California at Berkeley, Berkeley, CA 94720, USA
[5] Universität Hamburg, Sternwarte, Gojensbergweg 112, D-21029 Hamburg, Germany
[6] Astrophysikalisches Institut, An der Sternwarte 16, D-14482 Potsdam, Germany

Received 24 September 1998 / Accepted 10 December 1998

Abstract. Following the recent classification of the X-ray detected object V410 x-ray 3 with a young brown dwarf candidate (Briceño et al. 1998) and the identification of an X-ray source in Chamaeleon as young bona-fide brown dwarf (Neuhäuser & Comerón 1998), we investigate all ROSAT All-Sky Survey and archived ROSAT PSPC and HRI pointed observations with bona-fide or candidate brown dwarfs in the field of view with exposure times ranging from 0.13 to 221 ks, including dedicated 64 ks and 42 ks deep ROSAT HRI pointed observations on the low-mass star BRI 0021−0214 and the brown dwarf Calar 3, respectively. Out of 26 bona-fide brown dwarfs, one is newly detected in X-rays, namely ρ Oph GY 202. Also, four out of 57 brown dwarf candidates studied here are detected in X-rays, namely the young Taurus brown dwarf candidates MHO-4, MHO-5, V410 Anon 13, and V410 x-ray 3. The M9.5-type star BRI 0021−0214 is not detected. In the appendix, we also present catalogued, but as yet unnoticed B- and R-band data for some of the objects studied here.

Key words: X-rays: stars – stars: low-mass, brown dwarfs – stars: late-type

1. Introduction

Objects which are unable to sustain stable nuclear fusion of hydrogen, but which can burn deuterium until they are $\sim 10^7$ yrs old, are called brown dwarfs; see Kulkarni (1997) for a recent review. They continue to contract until electron degeneracy halts further contraction. Depending on metallicity and model assumptions made in for calculating theoretical evolutionary tracks, the limiting mass between normal stars and brown dwarfs is ~ 0.075 to $0.08\ M_\odot$ (Burrows et al. 1995, 1997, D'Antona & Mazzitelli 1994, 1997, Allard et al. 1997, Baraffe et al. 1998). Objects with masses below $\sim 0.01\ M_\odot$ cannot even burn deuterium and are called planets. One can also distinguish brown dwarfs from planets by the formation mechanism, namely objects formed in circumstellar accretion disks would be called planets, while those which formed by fragmentation of a protostellar cloud would be called brown dwarfs; however, we prefer to link the distinction with the physics going on inside the objects rather than with its formation, so that we regard all objects between ~ 0.01 and $0.08\ M_\odot$ as brown dwarfs, regardless of how they formed. One can identify an object as a brown dwarf either using the Lithium test (an object with primordial Lithium abundance either is very young or a brown dwarf or both, Rebolo et al. 1992) or by finding an object below the stellar limit in an H-R or color-magnitude diagram (for this, one needs to know the distance, eg., due to a bright stellar companion or confirmed membership of a cluster).

Because brown dwarfs have no stable nuclear energy source and derive most of their luminosity from gravitational contraction, they cool down and become less luminous as they age (Burrows et al. 1995, Brandner et al. 1997, Malkov et al. 1998). Hence, several search programs focused on zero-age main-sequence clusters and pre-main sequence associations. Eg., several brown dwarfs were discovered in the $\sim 10^8$ yr old Pleiades cluster (see Tables 1 and 2 for references). Briceño et al. (1998) could identify four brown dwarf candidates in the Taurus star forming region, one of which is V410 x-ray 3, a faint X-ray source detected by Strom & Strom (1994) and studied in detail also by Luhman et al. (1998). Several bona-fide and candidate brown dwarfs were found in ρ Oph (Rieke & Rieke 1990, Comerón et al. 1993, 1998a, Luhman et al. 1997, Wilking et al. 1999) and the Cha I dark cloud (Comerón et al. 1999, henceforth CRN99; Neuhäuser & Comerón 1998, NC98).

Here, we investigate on a statistically meaningful sample whether or not brown dwarfs emit X-rays. This sample consists of objects with largely differing properties, such as age, luminosity, temperature, and cluster membership. Thus, our study has the potential of exploring how X-ray properties are affected by all those factors.

Send offprint requests to: R. Neuhäuser (rne@mpe.mpg.de), co-authors are listed in alphabetical order

Table 1. Brown dwarfs (except Cha I).

Designation	$\log L_{bol}/L_\odot$	area	dist. [pc]	ref.
Roque 4	-3.35	Pleiades	125	1
MHObd3	-3.03	Pleiades	125	2
Roque 5	-3.45	Pleiades	125	3
Roque 13	-3.00	Pleiades	125	1
Roque 11	-3.15	Pleiades	125	1
Teide 1	-3.18	Pleiades	125	4,5
Roque 17	-2.83	Pleiades	125	1
Roque 16	-2.89	Pleiades	125	1,2,6
PPl 15	-2.80	Pleiades	125	7
Roque 12	-3.14	Pleiades	125	3
Roque 25	-3.90	Pleiades	125	3
Calar 3	-3.11	Pleiades	125	4,6
Teide 2	-2.90	Pleiades	125	8
CFHT-PL-18	-3.07	Pleiades	125	9,10
CFHT-PL-12	-2.82	Pleiades	125	6,9
CFHT-PL-15	-3.16	Pleiades	125	6,9
LP 944-20	-3.84	field	5	11,12
DenisJ1228−1547	-4.30	field	13	13,14
Kelu 1		field	≥ 12	15
CRBR 14	-1.52	ρ Oph	160	16,17
GY 10	-1.38	ρ Oph	160	16,17
GY 11 (*)	-2.63	ρ Oph	160	16,17
GY 64	-2.01	ρ Oph	160	16,17
GY 141	-2.36	ρ Oph	160	16
GY 202	-1.84	ρ Oph	160	16,17
GY 310	-1.20	ρ Oph	160	16,17

Remark: (*) L_{bol} is uncertain, because this object seems to be variable in the infrared (see Comerón et al. 1993, 1998a, Wilking et al. 1999).
References: (1) Zapatero-Osorio et al. 1997b, (2) Stauffer et al. 1998a, (3) Martín et al. 1998b, (4) Rebolo et al. 1995, (5) Rebolo et al. 1996, (6) Zapatero-Osorio et al. 1997a, (7) Basri et al. 1996, (8) Martín et al. 1998a, (9) Bouvier et al. 1998, (10) Martín et al. 1998c, (11) Kirkpatrick et al. 1997, (12) Tinney 1998, (13) Delfosse et al. 1997, (14) Martín et al. 1997, (15) Ruiz et al. 1997, (16) Comerón et al. 1993, (17) Wilking et al. 1999

In Sect. 2, we present the motivation for our study by elaborating on why brown dwarfs might be X-ray sources. In Sect. 3, we list all bona-fide and candidate brown dwarfs published so far (Tables 1 and 2), explain our X-ray data reduction procedures, list the ROSAT pointed observations with bona-fide or candidate brown dwarfs in the field of view (Table 3), and present the X-ray data for brown dwarfs and candidates (Tables 4 to 6) including the X-ray light curves for the two detected brown dwarf candidates with sufficient counts for a meaningful timing analysis. After comparing our results with those obtained by NC98 and CRN99 in Cha I (Sect. 4), we conclude with a brief discussion in Sect. 5.

2. Motivation

Any X-ray detection or low upper limit of a bona-fide brown dwarf would improve our currently incomplete understanding of brown dwarfs, and in particular it would help answering the question whether brown dwarfs support some mechanism ca-

Table 2. Brown dwarf candidates (except Cha I).

Designation	$\log L_{bol}/L_\odot$	area	dist. [pc]	ref.
PC 0025+0447	-3.74	field	60	18
296 A	-2.88	field	45	19
DenisJ0205−1159	-4.00	field	18	12
AP 270	-2.66	α Per	170	20,21
CFHT-PL-8	-2.87	Pleiades	125	8
CFHT-PL-17	-3.17	Pleiades	125	8
Roque 7	-3.31	Pleiades	125	8
CFHT-PL-20	-3.24	Pleiades	125	8
CFHT-PL-16	-3.01	Pleiades	125	8
MHObd4	-3.05	Pleiades	125	22
MHObd1	-2.90	Pleiades	125	22
CFHT-PL-19	-3.16	Pleiades	125	8
Roque 15	-2.86	Pleiades	125	1
Roque 14	-3.00	Pleiades	125	1
NPL 37	-3.22	Pleiades	125	23,24
MHObd5	-2.90	Pleiades	125	22
NPL 38	-3.24	Pleiades	125	23,24
PIZ 1	-3.39	Pleiades	125	25
NPL 36	-3.14	Pleiades	125	23,24
CFHT-PL-5	-2.71	Pleiades	125	8
NPL 40	-3.50	Pleiades	125	23,24
MHObd6	-2.85	Pleiades	125	22
CFHT-PL-1	-2.43	Pleiades	125	8
CFHT-PL-7	-2.86	Pleiades	125	8
CFHT-PL-6	-2.56	Pleiades	125	8
CFHT-PL-23	-3.27	Pleiades	125	8
CFHT-PL-2	-2.58	Pleiades	125	8
HHJ 22	-2.61	Pleiades	125	8,26
CFHT-PL-4	-2.65	Pleiades	125	8
CFHT-PL-26	-3.63	Pleiades	125	8
CFHT-PL-25	-3.42	Pleiades	125	8
CFHT-PL-22	-3.39	Pleiades	125	8
V410 x-ray 3	-1.21	Taurus	140	27,28
V410 Anon 13	-1.78	Taurus	140	28
Tau MHO-4	-1.37	Taurus	140	28
Tau MHO-5	-1.53	Taurus	140	28
RPr 1	-3.60	Praesepe	177	29
CRBR 15	-1.32	ρ Oph	160	15,16
GY 5	-1.14	ρ Oph	160	16
CRBR 28	-1.29	ρ Oph	160	15,30
CRBR 33	-1.52	ρ Oph	160	15,30
GY 31	-0.09	ρ Oph	160	16
GY 37	-1.56	ρ Oph	160	16
GY 59	-1.23	ρ Oph	160	16
GY 84	-0.93	ρ Oph	160	16
GY 107	-0.81	ρ Oph	160	16
GY 163	-0.69	ρ Oph	160	16
GY 218	-2.06	ρ Oph	160	15,30
GY 326	-0.64	ρ Oph	160	16
B185815.3−370435	-2.00	CrA	130	31
B185831.1−370456	-2.60	CrA	130	31
B185839.6−365823	-3.10	CrA	130	31
B185840.4−370433	-2.20	CrA	130	31
B185853.3−370328	-2.20	CrA	130	31
D04	-4.23	field	48	32
D07	-4.53	field	43	32
BRI 0021−0214	-3.50	field star	12	33

Table 2. (continued)

References: (1) to (17) as in Table 1, (18) Schneider et al. 1991, (19) Thackrah et al. 1997, (20) Prosser 1994, (21) Basri & Martín 1999, (22) Stauffer et al. 1998b, (23) Festin 1998a, (24) Festin 1998b, (25) Cossburn et al. 1997, (26) Hambly et al. 1993, (27) Luhman et al. 1998, (28) Briceño et al. 1998, (29) Magazzù et al. 1998, (30) Comerón et al. 1998a, (31) Wilking et al. 1997, (32) Hawkins et al. 1998, (33) Tinney et al. 1995.

pable of heating coronae. We recall that T Tauri stars and also optically invisible infrared Class I objects (protostars) display X-ray activity, despite the lack of a stable nuclear energy source (see Neuhäuser 1997 for a review). Gravitationally contracting low-mass pre-main sequence objects, at least those with spectral type M, are fully convective, and in some sense similar to young brown dwarfs which - by definition - never reach the main sequence, so that we may suspect young brown dwarfs to display X-ray emission via a similar mechanism.

While it is not clear whether brown dwarfs can drive and sustain a dynamo capable of heating coronae similar to low-mass stars, it is encouraging that some very old late-type stars are also detected in X-rays: vB 8 with spectral type M7 and a mass of $\sim 0.08\ M_{\odot}$ is clearly detected as an X-ray source (Fleming et al. 1993, Giampapa et al. 1996). Fleming et al. (in preparation) detected an X-ray flare of the M8-type star vB 10, which is not detected before and after the flare.

The low-mass object V410 x-ray 3 with spectral type M6-7, a mass of only $\leq 0.15\ M_{\odot}$, and an age of just ~ 1 Myr (Luhman et al. 1998) is clearly detected in X-rays (Strom & Strom 1994). The optical and infrared data by Luhman et al. (1998) have recently been re-evaluated by Briceño et al. (1998), who classify this object as brown dwarf candidate with a mass of 0.03 to $0.08\ M_{\odot}$ and an age of ≤ 0.9 to 1.5 Myr, depending on which evolutionary tracks and isochrones are used. The classification of this X-ray source as brown dwarf candidate shows that an object near the stellar burning limit can emit X-rays.

Recently, CRN99 have performed an $H\alpha$ objective prism survey as well as optical and infrared photometry of the Cha I dark cloud, a site of on-going low- and intermediate-mass star formation. They found three low-mass objects with infrared excess and six additional low-mass late-type objects with $H\alpha$ emission, all of which are near, and some possibly below the hydrogen burning limit. NC98 did follow-up spectroscopy with high S/N of the lowest-mass object, $Cha\,H\alpha\,1$, and estimated its spectral type to be M7.5-M8. Using IJHK photometry (CRN99) and a distance of 160 pc (ie., the mean of the HIPPARCOS distances of Cha I T Tauri stars, Wichmann et al. 1998), its location in the H-R diagram is below the hydrogen burning limit; a first comparison with evolutionary tracks and isochrones preliminary yielded an age of ~ 1 Myr and a mass of $\sim 0.04\,M_{\odot}$ (NC98), recently revised by CRN99 to an age of 0.4 ± 0.1 Myrs and a mass of $0.03 \pm 0.01\ M_{\odot}$.

NC98 found that this object is clearly detected in a 36 ks ROSAT pointed observation of the Cha I dark cloud. Two Cha I brown dwarf candidates are marginally detected, one is not resolved from a nearby star, and the other candidates, including all three with infrared excess, are undetected. Thus, there is evidence that young brown dwarfs show X-ray emission, and that it may be rewarding to engage in a wider survey.

Table 3. ROSAT pointings analyzed here.

no.	Pointing ID	Instr.	PI	exp. [s]
1	201077p	PSPC	Fleming	9065
2	000105p	PSPC	MPE	650
3	200008p - 0 / - 2	PSPC	Caillault	12985
4	200008p - - 2	PSPC	Caillault	696
5	200008p - - 3	PSPC	Caillault	45
6	200008p - - 4	PSPC	Caillault	121
7	200008p - - 5	PSPC	Caillault	722
8	200068p - 0 / - 1	PSPC	Rosner	39920
9	200068p - - 1	PSPC	Rosner	1307
10	200556p	PSPC	Stauffer	22456
11	200557p	PSPC	Stauffer	27648
12	200949p	PSPC	Feigelson	6098
13	200001p - 0 / - 1	PSPC	Strom	30077
14	201598p - 201602p	PSPC	Barwig	28973
15	201312p	PSPC	Zinnecker	2800
16	201025p	PSPC	Walter	5448
17	900353p	PSPC	Burrows	7718
18	201313p	PSPC	Zinnecker	4027
19	200443p	PSPC	Pye	20074
20	600043p	PSPC	Jones	53511
21	600127p	PSPC	Petre	17766
22	800301p / - 1	PSPC	Loewenstein	8917
23	700921p / - 1	PSPC	Turner	10306
24	200250p	PSPC	Schmitt	1897
25	200599p - 200625p	PSPC	Schmitt	30166
26	200045p - 0 / - 1	PSPC	Montmerle	32847
27	200493p - 0 / - 1	PSPC	Walter	7460
28	900002p	PSPC	Garmire	7761
29	202214h - 1 / - 2	HRI	Schmitt	63897
30	400764h	HRI	Halpern	17615
31	600256h	HRI	Kim	7339
32	600831h / - 1	HRI	Fabbiano	162066
33	600220h	HRI	Sarazin	8538
34	600940h	HRI	Hanlan	63877
35	202069h	HRI	Rosner	30193
36	202070h	HRI	Rosner	29283
37	201413h - 1	HRI	Harnden	24202
38	202068h	HRI	Rosner	28896
39	201414h - 1	HRI	Harnden	34160
40	202515h	HRI	Neuhäuser	42286
41	202156h	HRI	Neuhäuser	7698
42	201090h	HRI	Damiani	5150
43	201835h	HRI	Montmerle	51710
44	201618h - 1 / - 2	HRI	Zinnecker	5566
45	201834h / - 1 / - 2	HRI	Montmerle	77869
46	201709h - 201714h	HRI	Damiani	28031
47	201055h	HRI	Walter	3650
48	201395h / - 1	HRI	Walter	19641

Table 4. X-ray upper limits for undetected bona-fide brown dwarfs (except Cha I).

Object designation	Spec type	$W_\lambda(H\alpha)$ [Å]	$v \cdot \sin i$ $[km\ s^{-1}]$	ref.	FOV no.	exp. [ks]	X-ray counts	$\log L_X$ $[erg\ s^{-1}]$	$\log L_X/L_{bol}$
Roque 4	M9	≤ 5		1	PSPC 3-6,8,11	76.2	unresolved (a)		
MHObd3	M8	5.9		2	RASS	0.38	≤ 0.3	≤ 28.18	≤ -2.38
Roque 5	M9	≤ 8		3	PSPC 2-6,8,9	68.6	≤ 2.9	≤ 26.90	≤ -3.24
Roque 13	M7.5	10.5		1	PSPC 2-6,8,9,11	76.6	≤ 17.5	≤ 27.64	≤ -2.95
Roque 11	M8	5.8		1	PSPC 2-6,8-11	103.9	≤ 2.9	≤ 26.72	≤ -3.72
Teide 1	M8	6		4	PSPC 2-6,9-11	98.6	≤ 5.0	≤ 26.98	≤ -3.43
Roque 17	M6.5	15		1	RASS	0.36	≤ 0.3	≤ 28.20	≤ -2.56
Roque 16	M7	5		2	PSPC 2,3,5,6,8-11	94.1	≤ 3.8	≤ 26.89	≤ -3.75
PPl 15	M6.5	12:		5	PSPC 2,3,5-10	73.8	≤ 3.0	≤ 26.89	≤ -3.90
					HRI 38,39	59.4	≤ 42.1	≤ 28.61	≤ -2.18
Roque 12	M7.5	19.7		3	PSPC 2,5,6,8-11	68.3	≤ 3.0	≤ 26.92	≤ -3.53
Roque 25	L (c)	≤ 5		3	PSPC 2,7	0.80	≤ 3.6	≤ 28.93	≤ -0.76
Calar 3	M8	10		6	PSPC 2,3,8,10	16.3	≤ 4.7	≤ 27.74	≤ -2.74
					HRI 40	42.7	≤ 0.5	≤ 26.82	≤ -3.66
Teide 2	M6-7	7	13	2,6	PSPC 10	18.0	unresolved (a)		
CFHT-PL-18	M8			7	PSPC 7	0.37	≤ 2.7	≤ 29.14	≤ -0.82
CFHT-PL-12	M8	17		2	PSPC 7	0.27	≤ 7.1	≤ 29.70	≤ -1.07
					RASS (b)	0.37	≤ 4.0	≤ 29.31	≤ -1.46
CFHT-PL-15	M7	7		2	RASS (b)	0.36	≤ 0.3	≤ 28.20	≤ -2.23
LP 944-20	M9	1		8	PSPC 20-23	66.7	≤ 84.4	≤ 25.58	≤ -4.16
					HRI 31-34	220.8	≤ 91.6	≤ 25.57	≤ -4.17
DenisJ1228−1547	L (c)	≤ 1	20	9,10	RASS (b)	0.32	≤ 3.1	≤ 27.29	≤ -2.00
Kelu 1	L (c)	yes		9,11	RASS (b)	0.16	≤ 2.8	(d)	
CRBR 14	M7.5			12	PSPC 26	30.5	≤ 6.6	≤ 28.13	≤ -3.88
					HRI 43-46	148.0	≤ 3.9	≤ 27.69	≤ -4.32
GY 10	M8.5			12	PSPC 26 (e)	30.7	≤ 7.5	≤ 28.18	≤ -3.97
					HRI 43-46	148.0	≤ 3.6	≤ 27.65	≤ -4.50
GY 11 (f)	M6.5			12	PSPC 26	30.8	≤ 12.6	≤ 28.54	≤ -2.36
					HRI 43-46	148.0	≤ 3.2	≤ 27.60	≤ -3.30
GY 64	M8			12	PSPC 26	31.4	≤ 6.2	≤ 28.09	≤ -3.43
					HRI 43-46	148.0	≤ 13.0	≤ 28.21	≤ -3.31
GY 141	M8.5	60		12	PSPC 26 (g)	33.0	≤ 8.7	≤ 27.91	≤ -3.26
					HRI 43-46	148.0	≤ 11.5	≤ 27.86	≤ -3.31
GY 310	M8.5			13	PSPC 26 (h)	28.2	≤ 49.5	≤ 29.04	≤ -3.29
					HRI 45 (h)	76.5	≤ 7.9	≤ 28.28	≤ -4.05

References: (1) Zapatero-Osorio et al. 1997b, (2) Stauffer et al. 1998a, (3) Martín et al. 1998b, (3) Rebolo et al. 1995, (5) Martín et al. 1996, (6) Martín et al. 1998a, (7) Martín et al. 1998c, (8) Tinney 1998, (9) Martín et al. 1997, (10) Tinney et al. 1997 (11) Ruiz et al. 1997, (12) Wilking et al. (1999), (13) Luhman et al. 1997.

Remarks: (a) Located in the wing of a bright X-ray source, hence a very large upper limit. (b) RASS data are listed, if the object is not located in any pointed observation, which is significantly deeper than the RASS exposure. (c) New spectral type L for low-luminosity objects with spectral type later than M as suggested by Martín et al. (1997) and Kirkpatrick et al. (1998). (d) Distance as yet unknown. (e) Listed as possible, X-ray detected ρ Oph cloud member in Casanova et al. (1995), as also mentioned in Wilking et al. (1999), but located more than one arc minute away from the X-ray source, so that the identification is dubious; we cannot confirm the X-ray detection. (f) Luminosities are uncertain, because this object seems to be variable in the infrared (see Comerón et al. 1993, 1998a, Wilking et al. 1999). (g) Slightly lower upper limit reported earlier by Luhman et al. (1997), obtained from the 1 σ noise level in the hard band ROSAT map published by Casanova et al. (1995). (h) Upper limits are large, because GY 310 is located in the wing of the bright X-ray source ROXR1 50 (Casanova et al. 1995), also detected by the *Einstein Observatory* as source ROX 20 (Montmerle et al. 1983), identified with the classical T Tauri star GY 314.

In addition, two of the brown dwarf candidates in ρ Oph recently presented by Wilking et al. (1999), namely GY 5 and GY 37, are listed as tentative counterparts to X-ray sources by Casanova et al. (1995), as already mentioned by Wilking et al. (1999).

There are two more motivations for studying whether brown dwarfs can emit X-rays, namely: First, Pravdo et al. (1996) argue from the low X-ray luminosity of the 51 Peg system that the companion to 51 Peg is a planet. If 51 Peg B would be a close stellar companion, they argue, then one would expect stronger X-ray emission. However, they also come to the conclusion that the upper mass limit of 51 Peg B is $\sim 10\ M_{jup}$, so that – depending on the distinction between giant planets and brown dwarfs – 51 Peg B may either be a brown dwarf or a planet.

Table 5. X-ray detected bona-fide brown dwarfs (BD) and candidate brown dwarfs (BDC) (except Cha I).

Designation (Spec type)	FOV no. (1)	X-ray position α_{2000}	δ_{2000}	off-set	ML (2)	exp. [ks]	hardness ratios $HR\,1$	$HR\,2$	X-ray counts	$\log L_X$ $[erg\ s^{-1}]$	$\log L_X/L_{bol}$
GY 202	P26 (3)	16:27:04.6	-24:28:36.7	19″	8.5	31.6	≥ -0.17	0.86 ± 0.64	7.9 ± 5.9	28.19	-3.50
(M7) BD	H43-46		not detected			148.0			≤ 13.6	≤ 28.23	≤ -3.46
V410 x-ray 3	P13 (4)	04:18:08.4	28:26:00.3	7″	77.1	29.8	0.90 ± 0.23	0.00 ± 0.16	60.6 ± 9.7	28.68	-3.70
(M6-6.5) BDC	H40		not detected			6.8			≤ 9.4	≤ 28.99	≤ -3.39
V410 Anon 13	P13	04:18:18.1	28:28:40.4	12″	11.4	29.9	≥ 0.05	0.72 ± 0.39	11.5 ± 6.7	28.26	-3.55
(M6-6.5) BDC	H40		not detected			6.9			≤ 2.1	≤ 28.63	≤ -3.18
Tau MHO-4	P17-19	04:31:24.2	18:00:22.3	3″	94.0	26.3	≥ 0.68	-0.12 ± 0.14	82.3 ± 13.0	28.87	-3.35
(M6-6.5) BDC	H41		not detected			4.7			≤ 8.9	≤ 29.13	≤ -3.09
Tau MHO-5	P17-19	04:32:15.2	18:12:47.4	12″	7.0	22.9	≥ 0.29	0.15 ± 0.39	14.4 ± 5.7	28.17	-3.89
(M6-6.5) BDC	H41		not detected			4.9			≤ 2.6	≤ 28.57	≤ -3.49

Remarks: (1) P for PSPC, H for HRI. (2) ML is maximum likelihood of existence (see text). (3) Not listed in Casanova et al. (1995) because of the low S/N ratio, but with $ML = 8.5$, ie. $4\,\sigma$ significance, the source probably is not spurious. (4) Different data reported by Strom & Strom (1994) and quoted in Luhman et al. (1998), but Preibisch & Zinnecker (1994) noted inconsistencies in the data reduction of Strom & Strom (1994).

Because it is not at all clear whether brown dwarfs usually emit X-rays, the conclusion drawn by Pravdo et al. (1996) may not be correct. If brown dwarfs can emit X-rays, the nature of 51 Peg B would remain unclear. Secondly, De Paolis et al. (1998) argued that Massive Astrophysical Compact Halo Objects (MACHOs) are dark clusters of brown dwarfs, which emit X-rays and can therefore be responsible for some part of the observed diffuse X-ray background.

3. The ROSAT data

In this study, we include only isolated brown dwarfs, ie. brown dwarfs which are not companions to normal stars. Hence, we include PPl 15, a double-lined spectroscopic binary consisting of two brown dwarfs (Basri & Martín 1998), and also the visual binary CFHT-Pl 18, where both companions are brown dwarfs (Martín et al. 1998c). Brown dwarf companions to normal stars are all close to their primary stars (a few arc seconds or less); and because all these primaries have late spectral types, they are all X-ray bright stars, so that possible X-ray emission from their brown dwarf companions cannot be resolved with the ROSAT Positional Sensitive Proportional Counter (PSPC) or the High Resolution Imager (HRI), although the latter offers a spatial resolution of ~ 4 arc seconds. For details on ROSAT and its instruments, the PSPC and the HRI, we refer to Trümper (1982), Pfeffermann et al. (1988), and David et al. (1996), respectively. Even the recently detected brown dwarf companion 16 arc seconds south-west of G 196-3 (Rebolo et al. 1998), which has been observed with the PSPC in the ROSAT All-Sky Survey (RASS), is not resolvable as possible faint X-ray source from its primary, an X-ray bright star listed in the ROSAT Bright Source Catalog (Voges et al. 1996).

In Tables 1 and 2, we list 26 previously published brown dwarfs and 57 brown dwarf candidates, respectively, sorted by right ascension in each group, with designation, bolometric luminosity, distance, and references. The Cha I objects are excluded here, because they were studied in CRN99 and NC98. In the last line of Table 2, we also list BRI 0021−0214, which is not a brown dwarf, but an M9.5 star included in our study, because it rotates particularly fast (Basri & Marcy 1995), which might induce strong X-ray emission due to a rotation driven dynamo effect. We have recently obtained a new, 64 ks ROSAT HRI observation centered on BRI 0021−0214. Bolometric luminosities L_{bol} as given in Table 2 for objects in CrA as well as for CRBR 28 and 33 in ρ Oph are calculated as in Comerón et al. (1998a), scaled to 130 pc (160 pc) distance for CrA (ρ Oph) and include a correction for foreground extinction. The L_{bol} values for the Hawkins et al. objects (the last two field brown dwarf candidate entries in Table 2; their third object, D12, is omitted here, because a spectrum taken by Martín & Basri, in preparation, shows that it is not a brown dwarf) are calculated from their J magnitudes in the near-IR, assuming a bolometric correction of $B.C. = -2$ at J (see Lawson et al. 1996 and references therein), based on the the extremely late spectral types indicated by their infrared colors. At J, the correction is not affected by any important absorption features, even for temperatures well below 2000 K, as observed in Gl 229 B, which ensures a smooth behavior of B.C. as a function of temperature (see Allard et al. 1997, Allard & Hauschildt 1995). Even for a spectral type later than M9, it is not likely to be off by more than 0.1 mag. L_{bol} for Pleiades objects with *MHO* designation as well as for Roque 5, 12, and 25 are estimated as in Zapatero-Osorio et al. (1997b).

In Table 3, we list all the ROSAT PSPC (first group) and HRI (second group) pointed observations analyzed here (sorted by right ascension in each group); we assign a running number (to be used in Tables 4 to 6) and list also the official pointing ID, the instrument used, the Principle Investigator (PI), and the nominal exposure time.

We reduced all these pointings with the Extended Scientific Analysis Software (EXSAS, Zimmermann et al. 1994) version 98APR running under ESO-MIDAS version 97NOV. Whenever an object was found to be located in the field-of-view (FOV) of

more than one PSPC or HRI pointing, we merged the data sets (separately for the two instruments) to gain sensitivity. We performed standard local and map source detection in five different bands: soft (0.1 to 0.4 keV), hard 1 (0.5 to 0.9 keV), hard 2 (0.9 to 2.0 keV), hard (0.5 to 2.0 keV), and broad (0.1 to 2.0 keV). After merging the source lists, each source was again tested in the above mentioned five bands by a maximum likelihood source detection algorithm. Eg., a maximum likelihood of existence $ML = 14.3$ (or 5.9) corresponds to 5 (or 3) Gaussian σ detections. We have also reduced the RASS observations in a similar manner for all objects. The brown dwarf candidates V410 Anon 13 and V410 x-ray 3 are located near the bright X-ray source V410 Tau, in the center of PSPC pointing no. 13, but near the edge of pointing no. 12, 14, 15, and 16, so that the FWHM of the source V410 Tau would be too large in the merged data set; hence, for these two objects, we use only pointing no. 13.

For all sources detected with $ML \geq 7$ (ie. $\geq 3.5\ \sigma$), we have checked whether any of the brown dwarfs or candidates is located within one arc minute for RASS data, 30 arc seconds for PSPC data, or ten arc seconds for HRI data, according to their respective positional precision. One out of 26 bona-fide brown dwarfs is detected in X-rays, and four out of 57 brown dwarf candidates are detected. Hence, for all the undetected objects, we have calculated X-ray upper limits at the source positions (see Neuhäuser et al. 1995).

In Tables 4 and 6, we list the X-ray upper limits for bona-fide brown dwarfs and candidates, respectively, with object designations, running numbers (from Table 3) of the pointings in which the objects were observed (and/or RASS), effective exposure times, upper limits to the background subtracted broad band counts, upper limit X-ray luminosities, and the upper limit X-ray to bolometric luminosity ratios. In Table 4, we also list the spectral types, $H\alpha$ equivalent widths (positive if in emission), and projected rotational velocities for the bona-fide brown dwarfs, as these parameters might be related to X-ray activity.

In Table 5, we list the X-ray data of the detected objects, with object designations, spectral types, ROSAT pointing numbers, X-ray position (J2000.0), offsets between X-ray and optical position, effective exposure times, X-ray hardness ratios, background subtracted broad band counts, X-ray luminosities, and X-ray to bolometric luminosity ratios. Hardness ratios are X-ray colors defined as follows: If $Z_{s,m,h}$ are the count rates in the bands soft (0.1 to 0.4 keV), medium (0.5 to 0.9 keV), and hard (0.9 to 2.0 keV), respectively, then

$$HR\,1 = \frac{Z_h + Z_m - Z_s}{Z_h + Z_m + Z_s} \quad \text{and} \quad HR\,2 = \frac{Z_h - Z_m}{Z_h + Z_m}$$

Ie., hardness ratios range from -1 to $+1$. If no counts are detected, e.g, in the soft band, then $HR\ 1 = 1$, but one can estimate a lower limit to $HR\ 1$ by using the upper limit to the soft band count rate Z_s in the formula above.

To convert X-ray count rates to fluxes, one must divide the count rates by the appropriate energy conversion factor, depending on X-ray spectrum and instrument response. We assume that the X-ray emission of brown dwarfs is consistent with a one-temperature Raymond-Smith spectrum (Raymond & Smith 1977), a thermal spectrum from a hot, optically thin plasma of solar abundance. We use $1\ keV$, ie., $\sim 10^7\ K$, as temperature of the X-ray emitting plasma, which is typical for late-type stars (Neuhäuser et al. 1995, CRN99) and the X-ray detected brown dwarfs in Cha I (NC98). Because foreground absorption is negligible for most of our objects, we use an energy conversion factor of $10^{11}\ cts\ cm^2\ erg^{-1}$ for PSPC observations (note that the RASS has been obtained with the PSPC). For the bona-fide and candidate brown dwarfs in ρ Oph, however, absorption is not negligible, but typically a few mag (Comerón et al. 1998a, Wilking et al. 1999), so that we use an appropriately smaller energy conversion factor, namely $0.5 \cdot 10^{11}\ cts\ cm^2\ erg^{-1}$; except for GY 141, where absorption is negligible, namely $A_V \simeq 0$ mag (Comerón et al. 1998a). For the Taurus brown dwarf candidates, absorption is very low for all objects, but V410 Anon 13 (Strom & Strom 1994, Briceño et al. 1998, Luhman et al. 1998). For hard Raymond-Smith spectra, as assumed here, the energy conversion factor for HRI observations is roughly three times smaller than for PSPC data.

The detected bona-fide brown dwarf ρ Oph GY 202, initially suggested as brown dwarf candidate by Comerón et al. (1993, 1998a), was recently confirmed to be a very young (≤ 1 Myr) bona-fide brown dwarf by Wilking et al. (1999). The four X-ray detected brown dwarf candidates are all located in L1495E, a young star forming cloud in Taurus. None of the other relatively young and, hence, bright objects, located in ρ Oph and CrA, nor any of the Pleiades objects were detected, despite the long ROSAT PSPC pointed observations in these fields (up to $\sim$ 100 ks). In the case of the ρ Oph and CrA objects, this could be because they have large extinction (except GY 141), hence X-rays in the wavelength range available to ROSAT would be highly absorbed. On the other hand, the Pleiades brown dwarfs are two orders of magnitude older than the young Taurus and Cha I objects, so they could simply be too faint in X-rays. It is surprising that ρ Oph GY 202 is detected in spite of the strong extinction of $A_V = 13$ mag (Wilking et al. 1999). We detected only photons in the hard band (above $\sim 1\ keV$), consistent with strong extinction.

Among the bona-fide brown dwarfs, the lowest upper limit in terms of L_X is found for LP 944-20, namely $\log(L_X/erg\ s^{-1}) \leq 25.57$ (ie. $\log(L_X/L_{bol}) \leq -4.17$) with HRI observations of 221 ks in total; in terms of $\log(L_X/L_{bol})$, the lowest upper limit is found for ρ Oph GY 10, namely $\log(L_X/L_{bol}) \leq -4.50$ with HRI observations of 148 ks in total. As far as the brown dwarf candidates are concerned, the lowest upper limit in terms of L_X is found for NPL 37, namely $\log(L_X/erg\ s^{-1}) \leq 26.72$ (ie. $\log(L_X/L_{bol}) \leq -3.65$) with a 104 ks PSPC pointed observations; in terms of $\log(L_X/L_{bol})$, the lowest upper limit is found for ρ Oph GY 31, namely $\log(L_X/L_{bol}) \leq -5.81$ with HRI observations of 148 ks in total. For BRI 0021−0214, we found a lower limit of $\log(L_X/erg\ s^{-1}) \leq 25.41$, ie. $\log(L_X/L_{bol}) \leq -4.68$) in a 63 ks HRI observation.

There are now six X-ray detected brown dwarf candidates (four in Taurus, two in Cha I) and two detected bona-fide brown

Table 6. Upper limits for brown dwarf candidates.

Object designation	FOV no.	exp. [ks]	X-ray counts	$\log L_X$ $[erg\ s^{-1}]$	$\log L_X/L_{bol}$
PC 0025+0447	1 (1)	8.7	≤ 3.5	≤ 27.24	≤ -2.61
296 A	RASS	0.41	≤ 2.8	≤ 28.22	≤ -2.49
J0205−1159	RASS	0.36	≤ 2.6	≤ 27.34	≤ -2.25
AP 270	30	16.2	≤ 5.1	≤ 28.52	≤ -2.40
CFHT-PL-8	4,11	22.9	≤ 16.9	≤ 28.15	≤ -2.57
CFHT-PL-8	35	26.7	≤ 2.7	≤ 27.76	≤ -2.96
CFHT-PL-17	4,5,11	19.3	≤ 5.8	≤ 27.76	≤ -2.66
CFHT-PL-17	35	27.1	≤ 19.2	≤ 28.61	≤ -1.81
Roque 7	3-6,8,11	54.6	≤ 4.6	≤ 27.20	≤ -3.08
CFHT-PL-20	11	18.7	≤ 5.8	≤ 27.77	≤ -2.58
CFHT-PL-20	36	26.1	≤ 21.1	≤ 28.66	≤ -1.69
CFHT-PL-16	4,11	19.2	≤ 5.3	≤ 27.72	≤ -2.86
CFHT-PL-16	36	25.0	≤ 18.9	≤ 28.63	≤ -1.95
MHObd4	4,11	25.0	≤ 10.7	≤ 27.91	≤ -2.63
MHObd1	3-5,8,9,11	83.3	≤ 12.4	≤ 27.45	≤ -3.24
MHObd1	37	23.0	≤ 9.1	≤ 28.36	≤ -2.33
CFHT-PL-19	11	14.7	≤ 23.9	≤ 28.49	≤ -1.94
Roque 15	2-6,8,9,11	97.0	≤ 9.8	≤ 27.28	≤ -3.45
Roque 14	2-6,8,10,11	103.4	≤ 3.1	≤ 26.76	≤ -3.83
Roque 14	37	23.0	≤ 8.6	≤ 28.33	≤ -2.26
NPL 37	2-6,8-11	103.9	≤ 2.9	≤ 26.72	≤ -3.65
MHObd5	RASS	0.37	≤ 0.3	≤ 28.19	≤ -2.50
NPL 38	2,3,5-10	100.5	unresolved		
NPL 38	37,38	57.9	≤ 5.1	≤ 27.70	≤ -2.65
PIZ 1	2,3,8-11	56.8	≤ 7.0	≤ 27.37	≤ -2.83
NPL 36	2,3,5,6,8-10	77.7	≤ 3.0	≤ 26.87	≤ -3.58
CFHT-PL-5	2,3,8,10	55.0	≤ 2.8	≤ 26.99	≤ -3.89
NPL 40	2,3,6,8,9,11	82.9	≤ 8.3	≤ 27.28	≤ -2.81
MHObd6	2,3,8,10	63.7	≤ 6.0	≤ 27.25	≤ -3.49
CFHT-PL-1	2,10	13.7	≤ 4.4	≤ 27.78	≤ -3.38
CFHT-PL-1	40	40.3	≤ 10.5	≤ 28.17	≤ -2.99
CFHT-PL-7	2,7,10	17.6	≤ 11.2	≤ 28.08	≤ -2.65
CFHT-PL-6	10	15.3	≤ 19.1	≤ 28.37	≤ -2.66
CFHT-PL-6	40	38.0	≤ 4.1	≤ 27.73	≤ -3.30
CFHT-PL-23	7,10	12.4	≤ 5.6	≤ 27.93	≤ -2.39
CFHT-PL-2	7,10	14.2	≤ 2.7	≤ 27.56	≤ -3.45
HHJ 22	7,10	0.72	≤ 11.5	≤ 29.48	≤ -1.50
CFHT-PL-4	7,10	0.44	≤ 4.6	≤ 29.28	≤ -1.66
CFHT-PL-26	7	0.41	≤ 2.3	≤ 29.03	≤ -0.93
CFHT-PL-25	7	0.13	≤ 6.9	≤ 30.00	≤ -0.17
CFHT-PL-25	RASS	0.38	≤ 0.19	≤ 27.98	≤ -1.19
CFHT-PL-22	RASS	0.36	≤ 0.14	≤ 27.87	≤ -2.33
RPr 1	24,25	18.6	≤ 2.8	≤ 27.78	≤ -2.21
GY 5	26	30.5	≤ 8.6	≤ 28.24	≤ -4.15
GY 5	43-46	148.0	≤ 7.0	≤ 27.94	≤ -4.45
CRBR 28	26	31.9	≤ 7.7	≤ 28.17	≤ -4.23
CRBR 28	43-46	148.0	≤ 6.8	≤ 27.93	≤ -4.46
CRBR 33	26	30.6	≤ 12.3	≤ 28.40	≤ -3.77
CRBR 33	43-46	148.0	≤ 4.6	≤ 27.76	≤ -4.41
GY 31	26	30.6	≤ 13.2	≤ 28.43	≤ -5.01
GY 31	43-46	148.0	≤ 3.4	≤ 27.63	≤ -5.81
GY 37	26 (2)	31.4	≤ 8.2	≤ 28.21	≤ -3.76
GY 37	43-46	148.0	≤ 5.8	≤ 27.86	≤ -4.01
GY 59	26	31.2	≤ 6.0	≤ 28.08	≤ -4.22
GY 59	43-46	148.0	≤ 6.8	≤ 27.93	≤ -4.37
GY 84	26	30.6	≤ 6.2	≤ 28.10	≤ -4.50
GY 84	43-46	148.0	≤ 11.1	≤ 28.14	≤ -4.46
GY 107	26	31.2	≤ 6.2	≤ 28.09	≤ -4.63
GY 107	43-46	148.0	≤ 15.6	≤ 28.29	≤ -4.43
GY 163	26	30.9	≤ 4.9	≤ 27.99	≤ -4.85
GY 163	43-46	148.0	≤ 33.8	≤ 28.63	≤ -4.21
GY 326	26	28.1	≤ 27.1	≤ 28.78	≤ -4.11
GY 326	45	76.3	≤ 5.5	≤ 28.13	≤ -4.76
B185815.3−370435	27,28	11.7	unresolved		
B185815.3−370435	47,48	18.0	≤ 3.3	≤ 28.04	≤ -3.55
B185831.1−370456	27,28	10.5	≤ 8.5	≤ 28.21	≤ -2.78
B185831.1−370456	47,48	18.0	≤ 3.2	≤ 28.03	≤ -2.96
B185839.6−365823	27,28	13.1	≤ 8.7	≤ 28.12	≤ -2.37
B185839.6−365823	47,48	18.3	≤ 3.5	≤ 28.06	≤ -2.43
B185840.4−370433	27,28	11.4	≤ 10.9	≤ 28.28	≤ -3.11
B185840.4−370433	47,48	17.7	≤ 5.9	≤ 28.30	≤ -3.09
B185853.3−370328	27,28	11.3	≤ 8.4	≤ 28.17	≤ -3.22
B185853.3−370328	47,48	17.9	≤ 6.3	≤ 28.32	≤ -3.07
D04	RASS	0.36	≤ 2.0	≤ 28.13	≤ -1.23
D07	RASS	0.25	≤ 3.3	≤ 28.51	≤ -0.55
BRI 0021−0214	29	63.2	≤ 3.1	≤ 25.41	≤ -4.68

(1) Similar upper limit reported by Fleming et al. (1993).
(2) Listed as possibly X-ray detected ρ Oph cloud member in Casanova et al. (1995), as also mentioned in Wilking et al. (1999), but it is located more than one arc minute away from the X-ray source, so that the identification is dubious; we cannot confirm the X-ray detection.

dwarfs. Out of those eight X-ray detected objects, only two have a S/N ratio of larger than 5, namely Tau MHO-4 (82.3 ± 13.0 counts) and V410 x-ray 3 (60.6 ± 9.7 counts), so that a meaningful timing analysis is possible. Tau MHO-4 is detected in three different pointings at slightly different count rates, namely 3.2 ± 1.0 cts/ks in the PSPC pointing no. 17 (PI Pye, obtained in March 1991), 5.9 ± 1.5 cts/ks in no. 18 (PI Zinnecker, Sept. 1992), and 3.0 ± 0.7 cts/ks in no. 19 (PI Burrows, Feb. 1993), indicating no variability above a $\sim 1\ \sigma$ level on a time-scale of months to years. There is no indication for variability for any of the other detected objects, nor in the undetected objects.

We display the X-ray light curves for Tau MHO-4 (PSPC pointing no. 19) and V410 x-ray 3 (PSPC pointing no. 13) in Figs. 1 and 2, respectively. No variability on a time-scale of hours can be detected in these light curves.

4. Comparison with Cha I

We list the X-ray data of the Cha I bona-fide brown dwarf (*Cha Hα 1*) and brown dwarf candidates from CRN99 and NC98 in Table 7, all of which are only $\sim 1\ Myr$ old. The X-ray luminosities of the three detected objects is $\sim 10^{28}\ erg\ s^{-1}$, the luminosity ratio $\log(L_X/L_{bol})$ is in the range -3.4 to -4.3. The data found for the four detected brown dwarf candidates in Taurus are very similar, the average in $\log\ L_X$ being 28.5 and in $\log(L_X/L_{bol})$ being -3.6, very similar also to *Cha Hα 1* and ρ Oph GY 202. This seems to be the typical X-ray emission level

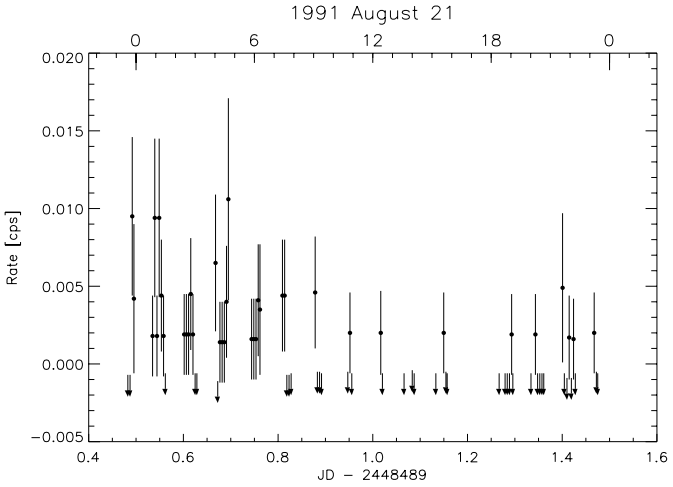

Fig. 1. X-ray light curve of V410 x-ray 3 with count rate in counts per second versus the observation time (JD date at the bottom axis, UT time on top axis), 400 s bins, 1 σ errors

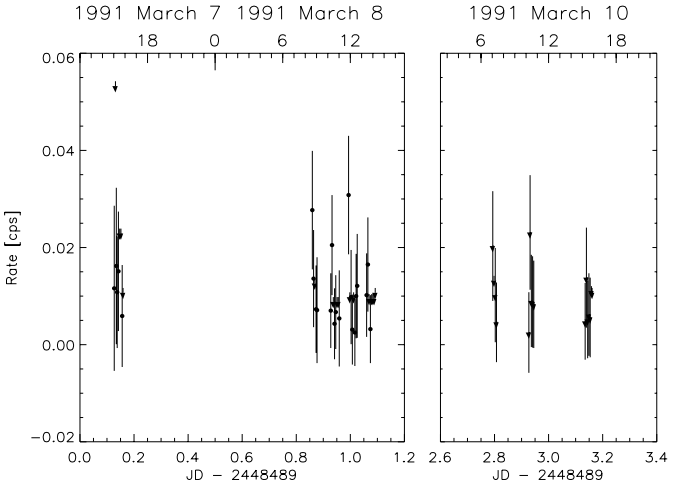

Fig. 2. X-ray light curve of Tau MHO-4 with count rate in counts per second versus the observation time (JD date at the bottom axis, UT time on top axis), 400 s bins, 1 σ errors

for such young, late-type, low-mass objects. Note that CRN99 have searched for brown dwarfs only in the center of the Cha I dark cloud, but nowhere else, so that there should be no strong bias towards the X-ray brightest low-mass objects in our Cha I sample.

Out of the 26 bona-fide brown dwarfs studied in this paper, 15 objects have an upper limit to the X-ray to bolometric luminosity ratio above the value found for $Cha\ H\alpha\ 1$, so that most of the non-detections found here may be due to too short X-ray exposures given the low optical/IR luminosities. The situation is similar for the brown dwarf candidates: Out of the 57 objects studied, 39 have an upper limit to L_X/L_{bol} above the value found for $Cha\ H\alpha\ 1$. See also Fig. 3 for a comparison of the upper limits found here with some X-ray detections.

Hence, although few of the ROSAT observations investigated here are deep enough to reach the L_X/L_{bol} values found for low-mass members of Cha I, we can conclude that the

Table 7. Cha I low-mass members.

Desig. CRN99	Spec type	exp. [ks]	X-ray counts	$\log L_X$ $[erg\ s^{-1}]$	$\log L_X/L_{bol}$	ref.
$H\alpha\ 1$	M7.5-8	37.8	31.4	28.41	-3.44	1,2
$H\alpha\ 2$	M6	not resolved, too close to another star				1,2
$H\alpha\ 3$	M6	37.6	11.9	27.99	-4.31	1,2
$H\alpha\ 4$	M6.5	34.8	≤ 22.9	≤ 28.31	≤ -4.91	1,2
$H\alpha\ 5$	M6	33.9	≤ 2.0	≤ 27.26	≤ -5.24	1,2
$H\alpha\ 6$	M6	31.8	8.2	27.90	-4.09	1,2
$IR\ 1$		30.7	≤ 4.7	≤ 27.68	≤ -4.37	2
$IR\ 2$		not resolved, too close to another star				2
$IR\ 3$		34.0	≤ 5.3	≤ 27.68	(3)	2

Remarks: (1) NC98, (2) CRN99. (3) L_{bol} as yet unknown. $H\alpha\ 1$ is a bona-fide brown dwarf (NC98), while the other objects are brown dwarf candidates (CRN99).

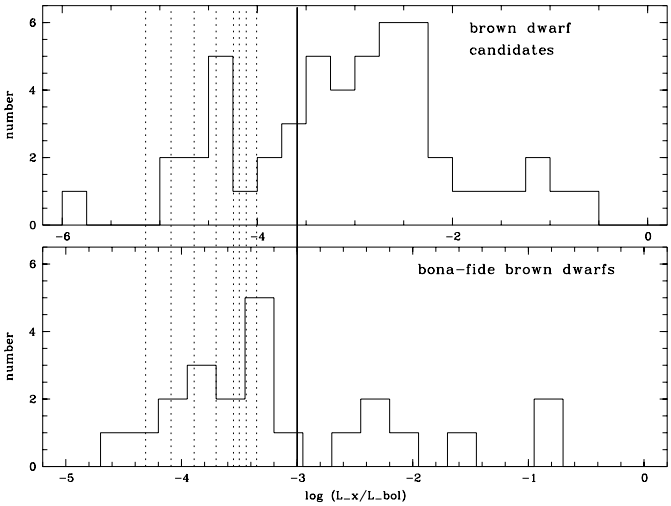

Fig. 3. Histogram of upper limits for $\log\ (L_X/L_{bol})$ for brown dwarf candidates (*upper panel*) and bona-fide brown dwarfs (*lower panel*). Dotted lines indicate the values of detected objects, namely from left to right $Cha\ H\alpha\ 3$, *6*, Tau MHO-5, V410 x-ray 3, V410 Anon 13, ρ Oph GY 202, $Cha\ H\alpha\ 1$, and Tau MHO-4 (with data from Tables 5 and 7). The X-ray saturation level is shown as full line. For objects with several upper limits available in Tables 4 or 6, we plot only the lowest limit

Pleiades brown dwarfs and candidates are X-ray fainter than the Cha I brown dwarfs. Even at the age of the Pleiades ($\sim 10^8$ yrs), brown dwarfs seem to be already too old, ie., too faint, to be detected in ~ 100 ks PSPC observations.

5. Discussion and conclusion

The $\log\ L_X/L_{bol}$ values for the detected objects lie intermediate between the brightest and faintest of the nine X-ray detected infrared Class I objects, which are EC 95 in Serpens with $\log\ L_X/L_{bol} = -2.0$ (Preibisch 1998) and TS 2.6 in CrA with $\log\ L_X/L_{bol} = -4.3$ (Neuhäuser & Preibisch 1997). T Tauri stars, though, typically have much larger X-ray luminosities, see Neuhäuser et al. (1995). X-ray saturation level for T Tauri stars

and X-ray active other stars is reached at $\log\ L_X/L_{bol} \simeq -3$. For most of the objects observed with pointed observations, the upper limits are below this value. Also, for all the objects in Chamaeleon and Taurus, the $\log\ L_X/L_{bol}$ values (or upper limits) lie below -3. For those objects, we can exclude that X-ray emission is saturated. We cannot exclude, though, that their X-ray emission is below the level of the quiet Sun being $\log\ L_X/L_{bol} \simeq -6$ (see Schmitt 1997). We find the same for BRI 0021−0214. The upper limit shows that its X-ray emission cannot be saturated, even though the fast rotation, but it still lies above the quiet Sun level. However, in the special case of ρ Oph GY 31, we find an upper limit of $\log\ L_X/L_{bol} \simeq -5.81$, ie. very close to the quiet Sun; this is more than an order of magnitude lower than for all other objects studied. The upper limits from both the PSPC and HRI observations are below -5. This is particularly surprising, because this object shows radio emission at 3.6 cm which may indicate non-thermal gyro-synchrotron emission due to magnetic field lines, in which hot, X-ray emitting plasma should be trapped. This radio emission, though, appears to be highly variable with 0.5 mJy in its high state and ≤ 0.1 mJy in its low state (P. André, private communication; incorrectly quoted in Wilking et al. 1999 as radio emission at 6 cm). It may be possible that all ROSAT observations of GY 31 took place during low-activity phases.

Canonical stellar evolution theory predicts that stars below $\sim 0.3\ M_\odot$ are fully convective (Drake et al. 1996). Hence, like low-mass late-type stars, brown dwarfs may emit X-rays; and in Cha I, one bona-fide brown dwarf and possibly two brown dwarf candidates are detected X-ray sources (NC98). However, convection alone is not enough to generate magnetic fields (and coronal X-ray emission). Some kind of rotation-induced dynamo is needed. Differential rotation could drive dynamo activity (α-ω dynamo) but convection implies rigid rotation and thus a solar-type dynamo should be quenched in completely convective stars (Drake et al. 1996). However, in the absence of differential rotation, another type of dynamo, related to the Coriolis force and driven by turbulent convection, can take over and cause coronal X-ray activity (α^2 dynamo).

If X-ray emission in brown dwarfs is driven by a dynamo, then it may be that only the fastest rotating brown dwarfs can be detected given the sensitivity of current instrumentation. Projected rotational velocities $v \cdot \sin i$ are known for two bona-fide brown dwarfs (see Table 4). They rotate relatively fast, but are not observed deeply with ROSAT (nor are they detected).

While an old star with a very late spectral type, like eg. M9, may in fact display weak coronal ($H\alpha$ and X-ray) activity, eg. due to low rotation, both young low-mass stars and young brown dwarfs with spectral types of late M or L can be fully convective and may then show X-ray emission. As the brown dwarf ages, fusion of deuterium in its center will stop, so that the temperature in its core will decrease. Consequently, the temperature gradient between center and surface will decrease and, hence, the convection velocity will decrease. Therefore, old brown dwarfs may not be able to show X-ray emission, even if they rotate fast, while old main sequence stars may still be able to produce X-rays.

Perhaps, the very low X-ray detection fraction of brown dwarfs is due to variability in the sense that brown dwarfs are no or very faint X-ray emitters for most of the time, but are in an high state for a time that is short compared to the typical exposure. However, it is unlikely that we would, by chance, detect X-ray emission from several brown dwarfs (or candidates) in Cha I and Taurus, while all Pleiades and field brown dwarfs remain undetected. Also, the X-ray detected objects in Cha I and Taurus do not show significant variability.

The X-ray detected brown dwarfs in Cha I may be close binaries with magnetic field configurations like in X-ray bright RS CVn-type binaries. However, it would be surprising that $Cha\ H\alpha\ 1$ (as a binary and being the X-ray brightest) is the faintest object in the optical among the six $H\alpha$ detected objects in Cha I (CRN99); if the other brown dwarf candidates in Cha I were close binaries, too, they should be brighter X-ray sources.

The X-ray emission may be linked to accretion or magnetic reconnection between the brown dwarf and a circumstellar disks, but no K-band near-IR excess is seen in the Cha I objects (CRN99). However, as far as $Cha\ H\alpha\ 1$ is concerned, excess emission is observed at 6.7 and 14.3 μm by ISOCAM with a color index $[14.3/6.7] = 0.15$ as in normal Class II objects (Comerón et al. 1998b); the fact that no excess is detected in the K-band is probably due to a very low accretion rate. Also, in the cases of ρ Oph GY 202 as well as Tau MHO-4 and MHO-5, some near-IR excess does indicate the presence of circumstellar material (Wilking et al. 1999; Briceño, unpublished).

$H\alpha$ emission, a proxy for chromospheric activity, might be related to X-ray emission. Two of the three X-ray detected objects in Cha I show strong $H\alpha$ emission with $W_\lambda(H\alpha) \simeq 60$ Å (CRN99), and also the four detected objects in Taurus show strong $H\alpha$ emission (Luhman et al. 1998, Briceño et al. 1998). However, the brown dwarf ρ Oph GY 141 shows similarily strong $H\alpha$ emission (Luhman et al. 1997), but no X-ray emission. $H\alpha$ emission is weak in most of the other bona-fide brown dwarfs (see Table 4).

X-ray emission of brown dwarfs, if typically present even in brown dwarfs as old as the Pleiades or older, may be similar to late-type low-mass stars, with $\log(L_X/L_{bol}) \simeq -4$. This cannot be rejected from our upper limits. However, it may be possible that only brown dwarfs younger than ~ 3 Myrs emit X-rays. Then, in contrast to normal stars, they get fainter and fainter in L_{bol} as they age (Burrows et al. 1995). Hence, their X-ray luminosity should also decrease. However, because low-mass objects like brown dwarfs probably have only weak or no winds, they have much longer time-scales for angular momentum loss compared to normal stars (Basri & Marcy 1995, Martín & Zapatero-Osorio 1997). Hence, if X-ray emission of brown dwarfs is due to a rotationally driven dynamo, as in other fully convective low-mass stars, then X-ray luminosities should decrease more slowly in brown dwarfs than in normal stars, so that the non-detection of Pleiades brown dwarfs would be surprising. We conclude that rotation is not the key parameter in X-ray emission of brown dwarfs. More important may be the fact that the convection velocity of brown dwarfs decreases significantly, because they become fainter as they age. Then,

one would also expect $H\alpha$ emission to be weaker in middle-aged and old brown dwarfs compared to young brown dwarfs. Indeed, strong $H\alpha$ emission is observed only in young brown dwarfs, but neither in Pleiades nor field brown dwarfs. From the X-ray detection of a few ~ 1 Myr young brown dwarfs and candidates and the undetection of the ~ 100 Myrs old Pleiades brown dwarfs, we may conclude that all the nearby field brown dwarfs and candidates, all undetected in X-rays, are too old and, hence, too faint for being detected in the long pointed observations, even though some of them may still rotate very fast. Eg., BRI 0021−0214 does rotate fast, but is undetected in X-rays and $H\alpha$ (Basri & Marcy 1995). Also, the old field brown dwarf DenisJ1228−1547 rotates fast, but shows weak or no $H\alpha$ emission (Tinney et al. 1997) as well as faint or no X-ray emission (see Table 4).

De Paolis et al. (1998) assumed that brown dwarfs display the same X-ray luminosity as very late-type stars like vB 8, ie. $\sim 10^{27}\,erg\,s^{-1}$. If MACHOs are clusters of brown dwarfs, then they could contribute for some part of the observed diffuse X-ray background. Here, we have obtained $\sim 10^{28}\,erg\,s^{-1}$ as typical X-ray emission level for young brown dwarfs. Although most of our upper limits do not reach below $10^{27}\,erg\,s^{-1}$, we do find significantly lower limits for BRI 0021−0214 and some bona-fide and candidate brown dwarfs. Hence, even if MACHOs are clusters of brown dwarfs, their contribution to the diffuse X-ray background may be lower than estimated by De Paolis et al. (1998).

With only a few detections (two bona-fide brown dwarfs and six candidates) and 81 upper limits, the X-ray luminosity function of brown dwarfs is not well constrained. However, there are still thousands of faint X-ray sources in deep ROSAT pointed observations, which remain to be identified.

Acknowledgements. We would like to thank Tom Fleming, Adam Burrows and Gibor Basri for useful discussion about X-ray emission of brown dwarfs. We are also grateful to Laurent Cambresy for pointing us to the USNO-PMM catalog. ROSAT is supported by the German government (BMBF/DLR) and the Max-Planck-Society. RN wishes to acknowledge financial support from the DFG Star Formation program. ELM was supported by a postdoctoral fellowship of the Spanish MEC.

Appendix A: B- and R-band data

We have cross-correlated the optical/IR positions of all bona-fide and candidate brown dwarfs studied here with the United States Naval Observatory (USNO) Precision Measuring Machine (PMM) catalog, which lists astrometric positions and photographic magnitudes in the blue (emulsion O or J) and red (emulsion E or F), all ± 0.5 mag (Monet 1996). Two of the objects listed above in Tables 1 and 2 are found in that catalog. The field brown dwarf candidate 296 A has $B = 21.0$ mag and $R = 17.8$ mag according to the USNO-PMM catalog; Thackrah et al. (1997) gave $R_F - I_N = 2.54 \pm 0.20$ mag with $I_N = 14.57 \pm 0.15$ mag. For the young Taurus brown dwarf candidate MHO-5, the USNO-PMM catalog lists $B = 18.9$ mag and $R = 15.7$ mag, whereas Briceño et al. (1998) gave $R_C = 16.23$ mag. Some of the Cha I low-mass objects are also listed in the USNO-PMM catalog (see note to Table 4 in CRN99). It may well be possible to find more brown dwarf candidates by cross-correlating the USNO-PMM catalog with other useful data bases like ROSAT source lists.

References

Allard F., Hauschildt P.H., 1995, ApJ 445, 433
Allard F., Hauschildt P.H., Alexander D.R., Starrfield S., 1997, ARA&A 35, 137
Baraffe I., Chabrier G., Allard F., Hauschildt P.H., 1998, A&A 337, 403
Basri G., Marcy G.W., 1995, AJ 109, 762
Basri G., Martín E.L., 1998, PPL 15: The first binary brown dwarf system? In: Rebolo R., Martín E.L., Zapatero-Osorio M.R. (eds.) Brown dwarfs and extrasolar planets. ASP Conf. Ser. 134, 284
Basri G., Martín E.L., 1999, ApJ 510, 266
Basri G., Marcy G.W., Graham J., 1996, ApJ 458, 600
Bouvier J., Stauffer J.R., Martín E.L., et al., 1998, A&A 336, 490
Brandner W., Alcalá J.M., Frink S., Kunkel M., 1997, The Messenger 89, 37
Briceño C., Hartmann L.W., Stauffer J.R., Martín E.L., 1998, AJ 115, 2074
Burrows A., Saumon D., Guillot T., Hubbard W.B., Lunine J.I., 1995, Nat 375, 299
Burrows A., Marley M., Hubbard W.B., et al., 1997, ApJ 491, 856
Casanova S., Montmerle T., Feigelson E.D., André P., 1995, ApJ 439, 752
Comerón F., Rieke G.H., Burrows A., Rieke M.J., 1993, ApJ 416, 185
Comerón F., Rieke G.H., Claes P., Torra J., Laureijs R.J., 1998a, A&A 335, 522
Comerón F., Neuhäuser R., Kaas A.A., 1998b, The Messenger 94, 28
Comerón F., Rieke G.H., Neuhäuser R., 1999, A&A, in press (CRN99)
Cossburn M.R., Hodgkin S.T., Jameson F., Pinfield D.J., 1997, MNRAS 288, L23
D'Antona F., Mazzitelli I., 1994, ApJS 90, 467
D'Antona F., Mazzitelli I., 1997, Evolution of Low Mass Stars. In: Micela G., Pallavicini R., Sciortino S. (eds.) Proceedings of the meeting on Cool stars in Clusters and Associations, Vol. 68 of the Mem. Soc. Astron. Italia conference series. Mem. Soc. Astron. Italia, Firence, 1997, pp. 807-822
David L.P., Harnden F.R., Kearns K.E., Zombeck M.V., 1996, The ROSAT High Resolution Imager calibration report. SAO technical report
Delfosse X., Tinney C.G., Forveille T., et al., 1997, A&A 327, L25
De Paolis F., Ingrosso G., Jetzer Ph., Roncadelli M., 1998, A&A 329, 74
Drake J.J., Stern R.A., Stringfellow G., et al., 1996, ApJ 469, 828
Festin L., 1998a, A&A 333, 497
Festin L., 1998b, MNRAS 298, L34
Fleming T., Giampapa M.S., Schmitt J.H.M.M., Bookbinder J.A., 1993, ApJ 410, 387
Giampapa M.S., Rosner R., Kashyap V., et al., 1996, ApJ 463, 707
Hambly N.C., Hawkins M.R.S., Jameson R.F., 1993, A&AS 100, 607
Hawkins M.R.S., Ducourant C., Jones H.R.A., Rappaport M., 1998, MNRAS 294, 505
Kirkpatrick J.D., Henry T.J., Irwin M.J., 1997, AJ 113, 1421
Kirkpatrick J.D., Cutri R.M., Nelson B., et al., 1998, BAAS 192, 5504
Kulkarni S.R., 1997, Sci 276, 1350
Lawson W.A., Feigelson E.D., Huenemoerder D.P., 1996, MNRAS 280, 1071

Luhman K.L., Liebert J., Rieke G.H., 1997, ApJ 489, 165
Luhman K.L., Briceño C., Rieke G.H., Hartmann L.W., 1998, ApJ 493, 909
Magazzú A., Rebolo R., Zapatero-Osorio M.R., Martín E.L., Hodgkin S.T., 1998, ApJ 497, L47
Malkov O., Piskunov A., Zinnecker H., 1998, A&A 338, 452
Martín E.L., Zapatero-Osorio M.R., 1997, MNRAS 286, L17
Martín E.L., Rebolo R., Zapatero-Osorio M.R., 1996, ApJ 469, 706
Martín E.L., Basri G., Delfosse X., Forveille T., 1997, A&A 327, L29
Martín E.L., Basri G., Gallegos J.E., et al., 1998a, ApJ 499, L61
Martín E.L., Basri G., Zapatero-Osorio M.R., Rebolo R., García López R.J., 1998b, ApJ 507, L41
Martín E.L., Basri G., Brandner W., et al., 1998c, ApJ Letters, in press
Monet D., 1996, BAAS 188, 5404 (see also http://vizier.u-strasbg.fr/cgi-bin/VizieR)
Montmerle T., Koch-Miramond L., Falgarone E., Grindley J.E., 1983, ApJ 269, 182
Neuhäuser R., 1997, Sci 276, 1363
Neuhäuser R., Comerón F., 1998, Sci 282, 83 (NC98)
Neuhäuser R., Preibisch Th., 1997, A&A 322, L37
Neuhäuser R., Sterzik M.F., Schmitt J.H.M.M., Wichmann R., Krautter J., 1995, A&A 297, 391
Pfeffermann E., et al., 1988, The focal plane instrumentation of the ROSAT telescope. In: Proc. SPIE 733, 519
Pravdo S.H., Angeli L., Drake S., Stern R., White N., 1996, New Astronomy 1 (2), 171
Preibisch Th., 1998, A&A 338, L25
Preibisch Th., Zinnecker H., 1994, A&A 292, 152
Prosser C., 1994, AJ 107, 1422
Raymond J.C., Smith B.S., 1977, ApJS 35, 419
Rebolo R., Martín E.L., Magazzù A., 1992, ApJ 389, L83
Rebolo R., Zapatero-Osorio M.R., Martín E.L., 1995, Nat 377, 129
Rebolo R., Martín E.L., Basri G., Marcy G., Zapatero-Osorio M.R., 1996, ApJ 469, L53
Rebolo R., Zapatero-Osorio M.R., Madruga S., et al., 1998, Sci 282, 1309
Rieke G.H., Rieke M.J., 1990, ApJ 362, L21
Ruiz M.T., Leggett S.K., Allard F., 1997, ApJ 491, L107
Schmitt J.H.M.M., 1997, A&A 318, 215
Schneider D.P., Greenstein J.L., Schmidt M., Gunn J.E., 1991, AJ 102, 1180
Stauffer J.R., Schultz G., Kirkpatrick J.D., 1998a, ApJ 499, L199
Stauffer J.R., Schild R., Barrado y Nacascues D., et al., 1998b, ApJ 504, 805
Strom K.M., Strom S.E., 1994, ApJ 424, 237
Thackrah A., Jones H., Hawkins M., 1997, MNRAS 284, 507
Tinney C.G., 1998, MNRAS 296, L42
Tinney C.G., Reid I.N., Gizis J., Mould J.R., 1995, AJ 110, 3014
Tinney C.G., Delfosse X., Forveille T., 1997, ApJ 490, L95
Trümper J., 1982, Adv. Space Res. 2 (4), 241
Voges W., Aschenbach B., Boller Th., et al., 1996, IAUC 6420
Wichmann R., Bastian U., Krautter J., Jankovics I., Ruciński S.M., 1998, MNRAS 301, L39
Wilking B.A., McCaughrean M.J., Burton M.G., et al., 1997, AJ 114, 2029
Wilking B.A., Greene T.P., Meyer M.R., 1999, AJ 117, 469
Zapatero-Osorio M.R., Rebolo R., Martín E.L., 1997a, A&A 317, 164
Zapatero-Osorio M.R., Rebolo R., Martín E.L., et al., 1997b, ApJ 491, L81
Zimmermann H.U., Becker W., Belloni T., et al., 1994, EXSAS Users's Guide, MPE Report 257, ROSAT Scientific Data Center, Garching